2012

Comparison of nanodosimetric parameters of track structure calculated by the Monte Carlo codes Geant4-DNA and PTra

P Lazarakis
University of Wollongong, pk97@uow.edu.au

M U. Bug
University of Wollongong, mb355@uowmail.edu.au

E Gargioni
Universit¨atsklinikum Hamburg-Eppendorf

S Guatelli
University of Wollongong, susanna@uow.edu.au

H Rabus
Physikalisch-Technische Bundesanstalt

See next page for additional authors

Comparison of nanodosimetric parameters of track structure calculated by Geant4-DNA and PTB Monte Carlo Codes

P Lazarakis[1,2], M U Bug[2,1], E Gargioni[3], S Guatelli[1], H Rabus[2] and A B Rosenfeld[1]

[1] Centre for Medical Radiation Physics (CMRP), University of Wollongong, NSW, Australia

[2] Physikalisch-Technische Bundesanstalt (PTB), Braunschweig, Germany

[3] Universitätsklinikum Hamburg-Eppendorf (UKE), Hamburg, Germany

Corresponding author:

Peter Lazarakis: Permanent address: EEC (CMRP), University of Wollongong, Northfields Av, Wollongong NSW 2519, Australia. pk97@uowmail.edu.au

Phone: +61 24221 4281

short title: Comparison of alternative Monte Carlo track structure codes

Index Terms: Radiotherapy, nanodosimetry, secondary electrons, Geant4, Monte Carlo, cluster size, low energy electrons, DSB, SB

ABSTRACT

The concept of nanodosimetry is based on the assumption that initial damage to cells is related to the number of ionisations (the ionisation cluster size) directly produced by single particles within, or in the close vicinity of, short segments of DNA. The ionisation cluster size distribution and other nanodosimetric quantities, however, are not directly measurable in biological targets and our present knowledge is mostly based on numerical simulations of particle tracks in water, calculating track structure parameters for nanometric target volumes. The assessment of nanodosimetric quantities derived from particle-track calculations using different Monte Carlo codes plays therefore an important role for a more accurate evaluation of the initial damage to cells and, as a consequence, of the biological effectiveness of ionising radiation. The aim of this work is to assess the differences in the calculated nanodosimetric quantities obtained with Geant4-DNA as compared to those of an *ad-hoc* particle-track Monte Carlo code developed at PTB. The comparison of the two codes was done for incident electrons of energy in the range between 50 eV and 10 keV, for protons of energy between 300 keV and 10 MeV, and for alpha particles of energy between 1 MeV and 10 MeV. Good agreement was found for nanodosimetric characteristics of track structure calculated in the high energy range of each particle type. For lower energies, significant differences were observed, most notably in the estimates of the biological effectiveness The largest relative differences obtained were over 50 %, however generally the order of magnitude was between 10 % and 20 %.

1. INTRODUCTION

Monte Carlo (MC) simulation became an established tool for radiation transport calculations over the last decades. Condensed history methods based on multiple scattering theories enable radiation transport MC codes, for instance, to compute the absorbed dose distribution in a macroscopic volume. MC techniques also proved successful in studying the microscopic track structure of ionising radiation, i.e. the spatial distribution of all interaction events of a primary particle and its secondary electrons (including delta electrons and all subsequent generations of electrons produced). Unlike condensed-history codes, in which many interactions linked to small changes of direction of momentum and energy (up to a few eV) are subsumed into an artificial event associated with a larger change in energy (typically keV) and direction, track structure codes simulate the transport of all particles step-by-step. Each single interaction is treated individually, where the average distance between loci of subsequent interactions is in the order of nanometres for a charged particle travelling in condensed matter.

Track structure codes have been employed to evaluate the risk of ionising radiation on human health by relating track structure characteristics to the damage to the DNA molecule, which is considered to be the most radiosensitive target in cells (Nikjoo and Goodhead 1991, Goodhead 2006, Nikjoo *et al* 2006, Schulte *et al* 2008). Interactions of ionising radiation within, or close to, the DNA molecule may result in damage in the form of DNA strand breaks (Bedford 1991, Goodhead *et al* 1993, Goodhead 2006, Garty *et al* 2010). Clusters of strand breaks can result in genomic instability, carcinogenesis, and cell death (Goodhead *et al* 1993, Goodhead 1994). The DNA molecule suffers the most severe damage from radiation characterized by a high linear energy transfer (LET) as found in space and aviation as well as in radiation therapy using any kind of particles. A high LET is an attribute of heavy ions, alpha particles and low energy protons, as well as of low energy electrons, which are produced in the slowing down process of

any radiation. With increasing LET, the number of energy deposition events per path length increases. This involves, among other processes, a higher number of ionisation events within small segments of DNA and, as a biological consequence, a high number of DNA strand breaks (Grosswendt 2005, Schulte *et al* 2008). Commonly, a double strand break (DSB) is defined as two strand breaks occurring on opposite DNA strands at a distance of up to 10 base pairs (Grosswendt 2002). Additional strand breaks within the same DNA segment increase the complexity of a DSB and, consequently, the repair becomes more error prone. Therefore, high-LET radiation has a high probability to produce clustered DNA damage in the form of complex DSB, resulting in a high biological effectiveness.

For nanometric targets, such as DNA segments of a few base pairs length, the concept of absorbed dose is unsuitable for a direct measure of the initial DNA damage by ionising radiation, as it is a mean value of the energy deposited per mass in a macroscopic volume. Over such a macroscopic volume energy deposition events within nanometric volumes occur stochastically, according to the track structure of the radiation. Therefore, initial DNA damage is more likely to correlate with parameters derived from the track structure at nanometre resolution as obtained, for instance, by simulations using track structure codes.

Several track structure codes have been developed in the last years (Krämer and Kraft 1994, Grosswendt 2002, Valota *et al* 2003, Salvat *et al* 2006, Incerti *et al* 2010) to model the interactions of particles down to energies of few eV, for the purpose of studying the correlation between track structure and biological effects of radiation. Until the development of Geant4-DNA, nanodosimetric parameters of track structure (NPTS) based on the probability distribution of ionisation cluster sizes and their relation to radiation biology have only been investigated using the track structure Monte Carlo code developed at PTB (further referred to as PTB MC code) specifically for nanodosimetric applications (Grosswendt 2002, Grosswendt and Pszona

2002). While the statistical uncertainty of nanodosimetric quantities has been investigated (Bug *et al* 2010), the availability of two independent MC codes now opens now the possibility to study the differences in nanodosimetric parameters as calculated by the two codes. In a MC simulation, differences in calculated quantities may originate, for instance, from the physical models used to describe the particle transport in the medium of interest, from the uncertainties in the parameterisation of the underlying experimental interaction cross sections, and from the particle transport algorithms. For a detailed discussion on a comparison of different MC codes the reader may refer to the work of Dingfelder *et al* (2008). The influence of different cross section models implemented in the same MC code on calculated nanodosimetric quantities was partly investigated by Gargioni and Grosswendt (2007), but has not yet been fully assessed.

In this paper, we compared nanodosimetric parameters of track structure obtained using the Geant4-DNA and the PTB MC codes and systematically evaluated the effect of differences in the implementation of particle transport algorithms and physical models for the interaction cross sections of liquid water. Additionally, we used the simulation results obtained with the two codes to carry out a similar comparison for a nanodosimetric estimate of biological effectiveness. This estimate was derived using the model proposed by Garty *et al* (2006, Garty *et al* 2010) to predict the probability of producing a DSB in a DNA segment.

2. METHODS

2.1 Nanodosimetric quantities

2.1.1 Nanodosimetric parameters of track structure (NPTS)

A particle with radiation quality Q (which is defined by the type of particle and its energy) produces a characteristic structure of interaction events (track structure) when slowed down in a medium. In nanodosimetry, the unique track structure of a specific radiation quality Q is characterised by the probability distribution $P(\boldsymbol{\nu}|Q)$ of the ionisation cluster size $\boldsymbol{\nu}$, which is defined as the number of ionisations produced by a single particle track within a specified target volume (Grosswendt 2002, Grosswendt and Pszona 2002). In common practice, the target volume is assumed to be filled with and surrounded by liquid water (Nikjoo and Goodhead 1991, Grosswendt 2002, Schulte *et al* 2008). The probability distribution $P(\boldsymbol{\nu}|Q)$ describes the probability that exactly $\boldsymbol{\nu}$ ionisations are produced per primary particle of radiation quality Q. In general, this probability distribution is characteristic of the radiation quality Q. However it also depends on the material composition of the target volume and on the impact parameter of the primary particle with respect to the target volume.

Different quantities derived from the ionisation cluster-size distribution can be used as nanodosimetric parameters of track structure. One such parameter is the mean ionisation cluster size $M_1(Q)$, given by the first moment of the probability distribution:

$$M_1(Q) = \sum_{\nu=0}^{\infty} \nu \, P(\nu|Q) \tag{1}$$

This track structure parameter can be considered as the nanodosimetric equivalent of the mean lineal energy, widely used in microdosimetry (Grosswendt 2006).

2.1.2 Nanodosimetric estimates of biological effectiveness

A correlation of NPTS with the probability of strand break formation in a DNA segment was suggested by Grosswendt (2005). He proposed that the probability to form a DSB should be proportional to the cumulative probability $F_2(Q)$ for a radiation of quality Q to produce at least two ionisations within the volume of a DNA segment, as described by the following equation

$$F_2(Q) = \sum_{\nu=2}^{\infty} P(\nu|Q) \tag{2}$$

Despite supportive evidence for this hypothesis (Grosswendt 2007, Rabus and Nettelbeck 2011), the suggested proportionality is not by itself evident. A more sophisticated combinatorial approach was proposed by Garty *et al*. (2006, Garty *et al* 2010) to predict the frequency distribution of DNA strand breaks from the known ionisation cluster size distribution $P(\boldsymbol{\nu}|Q)$. The method is based on modelling the conditional probability $P(n_{\mathrm{sb}}|\boldsymbol{\nu})$ to obtain a cluster of single strand breaks (SB) of size n_{sb} when the ionisation cluster size is $\boldsymbol{\nu}$. This model relies on the probability p_{c} of one ionisation being converted into a SB (discussion about p_{c} follows below). By convoluting the probability distribution of ionisation cluster sizes with the conditional probabilities of an ionisation cluster of size $\boldsymbol{\nu}$ being converted into a SB cluster of size n_{sb}, one obtains the probability distribution of strand breaks for the given radiation quality Q:

$$P(n_{sb}|Q) = \sum_{\nu=0}^{\infty} P(n_{sb}|\nu)\, P(\nu|Q) \tag{3}$$

In a similar manner, the conditional probability $P(\mathrm{DSB}|n_{\mathrm{sb}})$ for a SB cluster of size n_{sb} to lead to a double strand break (DSB) allows one to obtain the total probability for DSB formation:

$$P(DSB|Q) = \sum_{n_{sb}=2}^{\infty} P(DSB|n_{sb})\, P(n_{sb}|Q) = \sum_{\nu=2}^{\infty} P(DSB|\nu)\, P(\nu|Q) \tag{4}$$

To derive the required conditional probabilities, this model (Garty *et al* 2006) is based on two assumptions. First, that the probability p_{c} of converting a single ionisation to a strand break is independent of the cluster size and of the location of the ion within the volume of the DNA

segment. Second, that a double strand break will be produced whenever breaks are present in this DNA segment on both strands of the DNA backbone. In this way, the conditional probability $P(n_{sb}|\boldsymbol{\nu})$ to obtain a SB cluster of size n_{sb} for a specific ionisation cluster size $\boldsymbol{\nu}$ is given by the binomial distribution $B(n_{sb}; \boldsymbol{\nu}, p_c)$, while the conditional probability $P(\mathrm{DSB}|n_{sb})$ that n_{sb} strand breaks will result in a DSB is given by

$$P(DSB|n_{sb}) = 1 - (0.5)^{n_{sb}-1} \tag{5}$$

In consequence, the resulting conditional probability $P(\mathrm{DSB}|\boldsymbol{\nu})$ for an ionisation cluster of size $\boldsymbol{\nu}$ to result in a DSB is

$$P(DSB|\nu) = 1 + (1 - p_c)^{\nu} - 2(1 - p_c/2)^{\nu} \tag{6}$$

Here, p_c is the constant probability for an ionisation to be converted into a strand break. This is an adjustable model parameter that is dependent on many conditions, such as the biological endpoint under study, cell type, DNA status (which depends on the cell cycle), as well as the geometry (size, shape, material) used in the simulations to determine the probability distributions of ionisations $P(\nu|Q)$. By fitting the predicted DSB formation probability to the results of a plasmid DNA assay, Garty *et al.* (2010) found a value for p_c of 11.7 %. However, for the purposes of comparing MC codes the precise value of p_c is not important, as long as the same value is used for all calculations.

The probability distribution of strand breaks, $P(n_{sb}|Q)$, as well as the probability of a radiation quality Q to cause a double strand break, $P(\mathrm{DSB}|Q)$ or $F_2(Q)$, can be used as nanodosimetric estimates of biological effectiveness. In this work, we determined the effect of using different MC codes (different transport methods and different physical interaction cross sections) on the calculation of these parameters for different radiation qualities.

2.2 Determination of nanodosimetric parameters

2.2.1 Track structure Monte Carlo simulation

To calculate NPTS by Monte Carlo simulations, the particles track structure has to be calculated such that secondary electrons histories are followed step-by-step until their energy falls below a threshold of a few eV. Such capability is possible with the PTB Monte Carlo track structure code and with Geant4-DNA. The PTB MC code was specifically developed and is well established for nanodosimetry (Grosswendt and Pszona 2002, Schulte *et al* 2008, Bashkirov *et al* 2009, Garty *et al* 2010). Geant4 is the only open-source, general-purpose Monte Carlo code system and the recently released Geant4-DNA Very Low Energy physical interaction models provide a potential capability for nanodosimetry applications (Agostinelli *et al* 2003, Allison *et al* 2006, Chauvie *et al* 2007, Incerti *et al* 2010). Because the Geant4-DNA software package is under development to refine its functionality, a regression test was performed, comparing Geant4 releases 9.2.p01, 9.2.p02 (including G4EMLOW 6.2) and 9.3 (including G4EMLOW 6.9) to check the consistency of the results deriving from the simulation through the evolution of the MC code. Results obtained by different versions of Geant4 in conjunction with different versions of low energy electromagnetic processes were compared and showed agreement, within the statistical uncertainties, for the calculated nanodosimetric parameters.

Detailed information on track structure simulations and the physical interaction cross section models adopted in both MC codes is provided in the appendix.

2.2.2 Geometrical set-up of the simulation study

Nanodosimetric parameters of track structure were determined in targets equal in volume to a DNA segment of 10 base pairs length and a nucleosome, both modelled as water cylinders with nanometric dimensions. This simplified modelling of the DNA using cylindrical volumes is a common practice in nanodosimetric simulations (Grosswendt 2002, Nikjoo and Goodhead 1991). Figure 1 illustrates the geometrical set-up of the MC simulations. The DNA segment was modelled as a water cylinder of 2.3 nm diameter and 3.4 nm height. This cylinder was set inside

another water cylinder with 6 nm diameter and 10 nm height, which is equivalent to the size of a nucleosome or to a volume within which hydroxyl radicals can reach the DNA by diffusion. Thus, this geometry is a simplified model for estimating the indirect effects of the ionising radiation on the DNA molecule (Nikjoo and Goodhead 1991, Grosswendt 2002). The axes of the DNA segment and nucleosome were aligned along the z-axis. The nucleosome model was set in the centre of the '*world'* volume, which was modelled as a water cube of 150 nm edge length.

The radiation field was simulated as a monoenergetic pencil beam, incident on the surface of the DNA segment at half the cylinders' height, as illustrated in Figure 1. A pencil beam was chosen (rather than a broad beam) to provide an identical initial condition, such as the same potential path length through the target volume, for each incident particle. At least 10^5 primary particles were simulated per initial particle energy. Simulations were carried out for primary electrons with energies from 50 eV to 10 keV, for protons with energies from 300 keV to 10 MeV, and α-particles with energies from 1 MeV to 10 MeV. These are the energy ranges that were available in both codes at the time this investigation was carried out (refer to Appendix for details of physical models of interaction used in the codes).

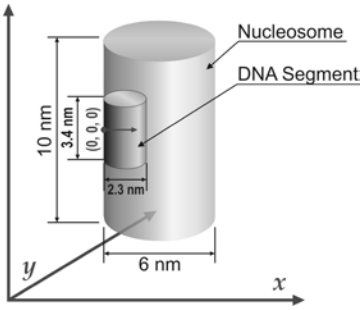

Figure 1. Geometrical set-up of the Monte Carlo simulations. The DNA segment and the nucleosome were embedded in a water cube of 150 nm edge length. The particle beam was incident on the surfaces on both cylindrical targets and directed along the x-axis.

2.2.3 Statistical uncertainty

We estimated the statistical uncertainty of the calculated nanodosimetric results in the following way: for each initial kinetic energy the relative frequency distribution of cluster size was used to calculate the corresponding cumulative probability distribution. These cumulative probabilities were then used as bin boundaries for binning sets of random numbers that were generated by a generator based on the AS183 algorithm (Wichmann and Hill 1982), which yields random numbers uniformly distributed between 0 and 1. For each cluster size distribution, 100 independent sets of at least 10^5 random numbers were used, such as to mimic 100 repetitions of our Monte Carlo simulations. For each set of random numbers, we determined the relative frequency distribution of ionisation cluster size $P(\nu|Q)$, the mean ionisation cluster size $M_1(Q)$, the probability $F_2(Q)$ for ionisation cluster sizes of at least two, the relative frequency distribution of SB cluster size $P(n_{sb}|Q)$ and the probability $P(\mathrm{DSB}|Q)$ for double strand breaks. For each of these quantities, the standard deviation u_i over the 100 repetitions was calculated and used as the statistical uncertainty estimate.

3. RESULTS AND DISCUSSION

3.1 Electrons

Figure 2 shows as an example the probability distribution of ionisation cluster sizes $P(\nu|Q)$ produced in both target volumes for incident electrons of 200 eV. The $P(\nu|Q)$ obtained in the DNA segment had a maximum at a cluster size of 1 and decreased with increasing cluster size. The maximum probability obtained in the nucleosome by the PTB and Geant4 simulations occurred at a cluster size of 6 and 8, respectively.

The probability for small cluster sizes (up to 5 for 200 eV electrons) was calculated by all simulations in good agreement. However, with the PTB simulation, a smaller number of large

cluster sizes were obtained than for the Geant4 simulations. The use of the two different physical models for elastic scattering available in Geant4-DNA resulted in a higher probability of large cluster sizes when the Screened Rutherford cross sections were used in comparison to those from Champions model (Champion 2003), which leads to significant discrepancies in the case of the DNA segment.

The variations between the results obtained by PTB and Geant4 simulations should be due to the different physical models for electron elastic and inelastic cross sections used in the codes. This conclusion is supported by the variation of the results obtained by Geant4, comparing both elastic scattering models.

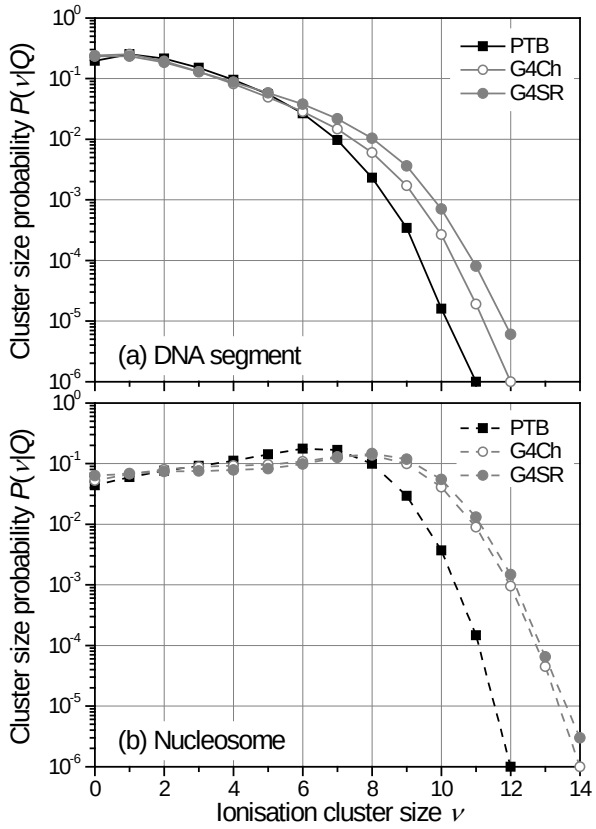

Figure 2. Probability distribution of ionisation cluster size $P(\nu|Q)$ in the DNA segment (a) and the nucleosome (b) obtained for incident electrons of 200 eV, calculated by means of the PTB and Geant4 MC codes by using the Screened Rutherford (G4SR) and the Champion model (G4Ch) for elastic scattering. Statistical error bars are not shown; for probabilities of approximately 10^{-5} and higher, the uncertainties are within the symbols. Below this value $P(\nu|Q)$ has relative statistical uncertainties of up to 100% (for the lowest probabilities).

Figure 3 shows the mean ionisation cluster size determined from $P(\nu|Q)$ for incident electron energies from 50 eV to 10 keV. The dependence of the mean ionisation cluster size on electron energy was described comprehensively by Bug *et al* (2010). Good agreement of all simulations was obtained for energies above 700 eV in the DNA segment and above 1 keV in the nucleosome. However, due to the variation of $P(\nu|Q)$ for large cluster sizes in the different simulations, smaller mean cluster sizes were obtained for lower energies with the PTB code, showing a relative difference of as much as 87 % at electron energies below 100 eV.

Furthermore, the Geant4 simulation using the Screened Rutherford elastic scattering model calculated larger mean cluster sizes for energies between 150 eV and 500 eV in the DNA segment and between 300 eV and 700 eV in the nucleosome. This is plausible if one considers the range $R_{0.95}$, that is the radius of a sphere containing 95 % of the ionisations produced by an electron until its complete slow down. In the afore mentioned energy ranges the cross sections for elastic scattering are large and the range of the electrons just exceeds the diameter of the respective target ($R_{0.95}$(150 eV) ≈ 6 nm, $R_{0.95}$(300 eV) ≈ 10 nm (Grosswendt 2002)). This leads to a higher probability that electrons are scattered out of the volume and deposit their energy in the surrounding medium. Our results show that the Screened Rutherford model allowed the particles to undergo a larger number of ionisations inside the targets than the Champion model. This is in direct relation to the difference in cross section for both models: the differential elastic scattering cross section for forward scattering is much larger in the Champion model than in the Screened Rutherford model and decreases dramatically for larger scattering angles (Champion 2003, Brenner and Zaider 1983). In addition, for electron energies between 150 eV and 700 eV, the total elastic scattering cross section for the Screened Rutherford model is up to 10 times larger than that of the Champion model (Champion 2003). These differences lead to a higher probability of electrons reaching the surrounding medium of the respective target in the Champion model, resulting in a lower number of ionisations within the target.

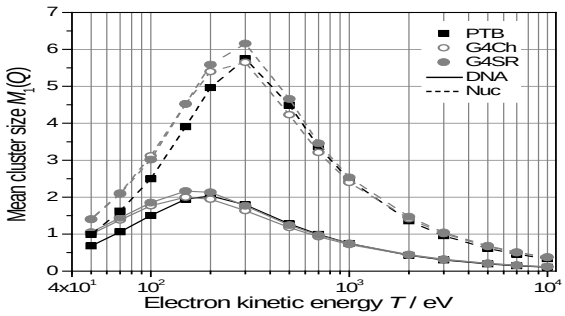

Figure 3. Mean ionisation cluster size $M_1(Q)$ as a function of incident electron energy T obtained in the DNA segment (DNA) and the nucleosome (Nuc) by the PTB simulation and Geant4, using the Screened Rutherford (G4SR) and the Champion model (G4Ch) for elastic scattering.

To investigate the influence of different Monte Carlo simulation codes on NPTS that are supposed to be related to biological effects (Grosswendt 2007), we calculated the probability $F_2(Q)$ that at least two ionisations are produced within a DNA segment according to Eq. (2). In good agreement to the mean cluster size, $F_2(Q)$ peaks at a maximum for electrons of 150 eV (Figure 4). Above 300 eV, we found good agreement between the results obtained from the different Monte Carlo simulations. A large difference, however, is observed for energies below 150 eV, where the value of $F_2(Q)$ determined from the PTB simulation is much smaller than that calculated by Geant4-DNA. This originates from the smaller probability of large cluster sizes in the DNA segment and from differences in $P(\nu|Q)$ already evident for cluster sizes of 3 or 4.

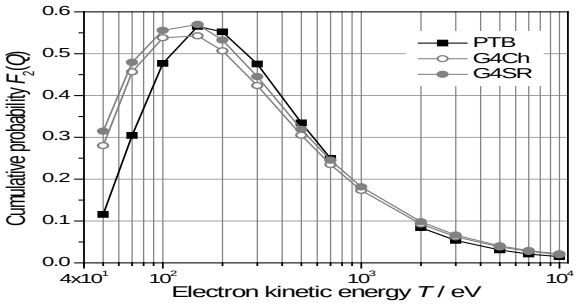

Figure 4.Cumulative probability, $F_2(Q)$, for electrons to produce at least two ionisations within the DNA segment, as a function of kinetic energy T, for PTB and Geant4 Monte Carlo simulations using the Screened Rutherford (G4SR) and the Champion model (G4Ch) for elastic scattering.

Figure 5 shows a comparison of the ionisation cluster size distributions, $P(\nu|Q)$, and the corresponding probability distributions for DNA strand breaks cluster size, $P(n_{sb}|Q)$, calculated using Eq (3); briefly, this combines $P(n_{sb}|\nu)$ with $P(\nu|Q)$ in a binomial distribution with the probability p_c = 11.7 % to determine $P(n_{sb}|Q)$. Discrepancies between the ionisation cluster size distributions that were present essentially for large ionisation cluster sizes have little impact on the SB distributions, where both codes provide very similar results. This implies that the biological damage predicted by the two codes will be very similar. The reason for this is that while the SB distribution depends strongly on the probabilities of producing large ionisation cluster sizes, here these probabilities take only low values of around 10^{-4} or less and so have only a minimal impact on $P(n_{sb}|Q)$.

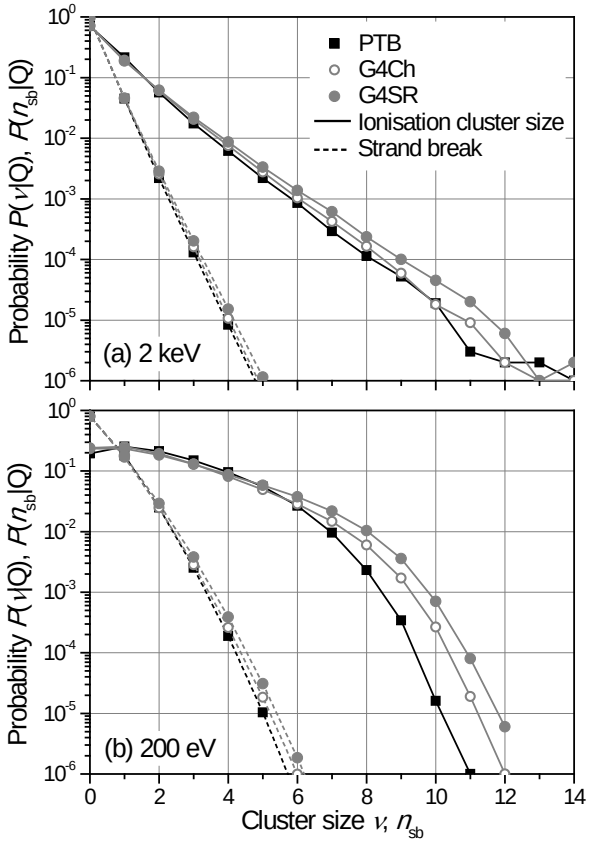

Figure 5. Probability distribution $P(\nu|Q)$ of ionisation cluster size, ν, in the DNA segment and probability distribution, $P(n_{sb}|Q)$, for DNA strand break cluster size, n_{sb}, for 2 keV (a) and 200 eV (b) electrons, calculated by means of the PTB and Geant4-DNA codes using the Screened Rutherford (G4SR) and the Champion model (G4Ch) for elastic scattering.

The probability of 200 eV electrons to produce a double strand break was (1.465 ± 0.003) % for Geant4-DNA (using Champion model) and (1.456 ± 0.003) % for the PTB code, where these uncertainties are statistical in origin. The small difference between the two codes is due to the slightly smaller values of the probabilities to produce two or more strand breaks, which occur for the PTB code.

The energy dependence of the probability to form a DSB is in agreement (within 30 %) for the two codes for electron energies above 200 eV (Figure 6). For lower energies, the PTB code predicts DSB production with consistently lower probability than Geant4-DNA. This indicates

that the two codes will predict similar amounts of biological damage for electron energies of 200 eV and above. Below this energy, Geant4-DNA will predict a higher amount of biological damage. This is in agreement with the values of both the mean ionisation cluster size and $F_2(Q)$.

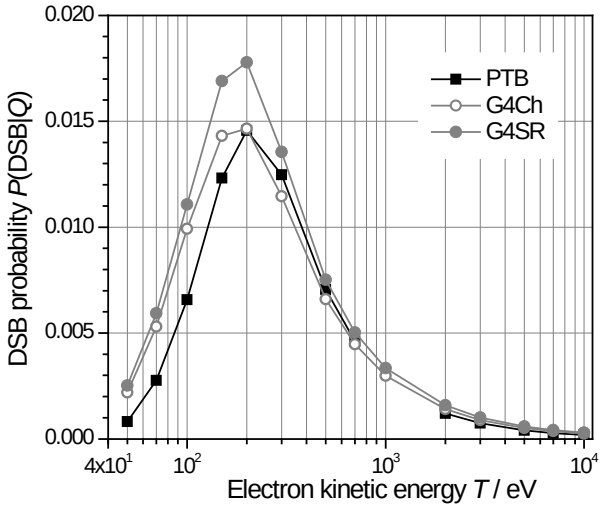

Figure 6. Probability of producing a DSB in the DNA segment as a function of kinetic energy, *T*, calculated by means of the PTB and Geant4 MC codes using the Screened Rutherford (G4SR) and the Champion model (G4Ch) for elastic scattering.

3.2 Protons and alpha particles

The probability distribution of ionisation cluster sizes *P(ν|Q)* produced in both target volumes is shown in Figure 7 for incident protons of 300 keV and incident alpha particles of 1 MeV, exemplarily. The *P(ν|Q)* obtained in the DNA segment for protons has a maximum at a cluster size of 2 and decreases with increasing cluster size. For alpha particles, the most frequent cluster size is 8 when simulations are performed with the PTB code, and 12 when using Geant4-DNA. The maximum probability obtained in the nucleosome for protons by the PTB and Geant4 simulations occurred at a cluster size of 6 and 8, respectively. For alpha particles a cluster size of 26 and 44 in the nucleosome had the maximum probability in the PTB and Geant4 simulations, respectively. All curves reach their maximum and then decrease with increasing cluster size. For

incident protons, the probability for very small cluster sizes (of around 2 or lower) was calculated by all simulations, for all energies, in good agreement. However the probabilities for producing large cluster sizes with the PTB simulations are systematically smaller than those of Geant4-DNA. These differences are significantly larger than the statistical uncertainties, which are not indicated in the figure as in most cases the error bars are within the symbols. For incident alpha particles, the maximum of the PTB curve is consistently higher than that of the Geant4-DNA curve, which predicts significantly higher probability for larger cluster sizes than the PTB code.

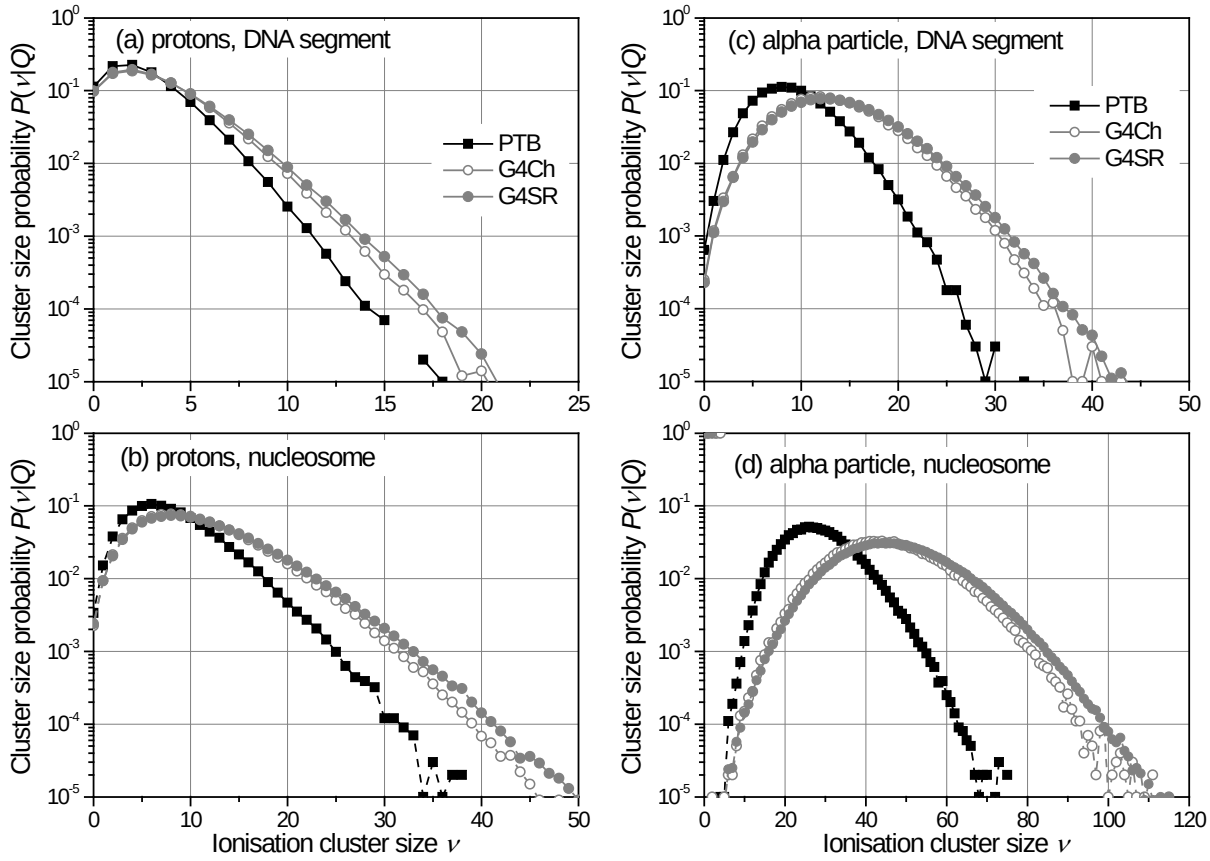

Figure 7. Probability distribution of ionisation cluster size for protons in the DNA segment (a) and the nucleosome (b) obtained for incident protons of 300 keV and incident alpha particles of 1 MeV (c) and (d), calculated by means of the PTB and Geant4 MC codes using the Screened Rutherford (G4SR) and the Champion model (G4Ch) for elastic scattering of the secondary electrons produced. Statistical error bars are not shown; for probabilities of

approximately 10^{-4} and higher, the uncertainties are within the symbols. Below this value $P(\nu|Q)$ has relative statistical uncertainties of up to 100% (for the lowest probabilities).

When comparing the different models used for elastic scattering of secondary electrons, namely the Screened Rutherford and Champion models, minor differences can be seen for very large ionisation cluster sizes (Figure 7). The reason for this is that the majority of secondary electrons produced by protons or alpha particles along their track are in an energy range where the electrons undergo strong scattering. Therefore only electrons produced in the vicinity of a nanometric volume may contribute to the number of ionisations produced therein. Figure 8 shows that for incident protons and alpha particles ionisations are mostly produced by the primary particle, with delta and other secondary electrons producing around 25 - 30% of the total number of ionisations in the DNA volume. The relatively small contribution of secondary electrons to the total number of ionisations implies that the large discrepancies between the PTB and Geant4 codes, as seen in Figure 7, cannot be explained by differences in electron interaction cross sections.

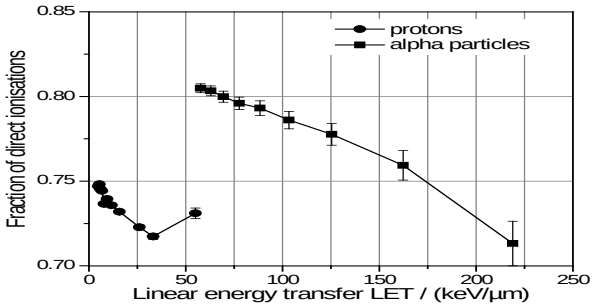

Figure 8. Fraction of ionisations in the DNA segment due to interactions of the primary particle, as a function of LET. Obtained for incident protons and alpha particles, calculated by means of Geant4-DNA using the Champion model for elastic scattering. LET values used here are the unrestricted LET obtained from NIST databases ASTAR and PSTAR (Berger *et al* 2005)

The discrepancies between the results obtained by PTB and Geant4 simulations may rather be due to the different physical models for ion cross sections used in the codes (refer to appendix). This is also supported by Figure 9 from which it can be deduced that the differences in the mean cluster size for protons and alpha particles between the two codes is too large to be due entirely, or even primarily, to differences in electron models.

Figure 9 shows the mean ionisation cluster size determined from $P(\nu|Q)$ for incident proton energies from 0.3 MeV to 10 MeV and incident alpha particles from 1 MeV to 10 MeV. For protons, the best agreement of all simulations is obtained for energies of 2 MeV and above in both the DNA and nucleosome volumes. However, due to the variation of $P(\nu|Q)$ for large cluster sizes in the different simulations (as seen in Figure 7), smaller mean cluster sizes are obtained for lower energies with the PTB code, showing a relative difference of as much as 31 % at proton energies below 1 MeV. We should note here that as the energy of the primary proton beam is decreased, the LET of the primary particles increases, so that the largest differences between the two codes are seen in the highest LET range. As the LET is increased, the number of secondary electrons produced will also increase.

For incident alpha particles, we found good agreement between the Geant4-DNA and PTB codes for energies of around 3 MeV and above. Below this limit, the PTB code produces consistently lower mean ionisation cluster sizes than those obtained by Geant4-DNA with differences of as much as 60% between the two codes. This is consistent with the larger ionisation cluster sizes scored by Geant4-DNA as observed in the cluster size probability distributions in Figure 7. The variations between the results obtained by PTB and Geant4-DNA simulations may be due to the different physical models for alpha particle interaction cross sections used in both codes. As with the proton results, this is demonstrated in part in Figure 9. In fact, changing the elastic scattering model for electrons had only a small effect on the simulation, whereas the different models for

alpha particle interactions applied in the MC codes produces a much larger difference between the mean ionisation cluster sizes.

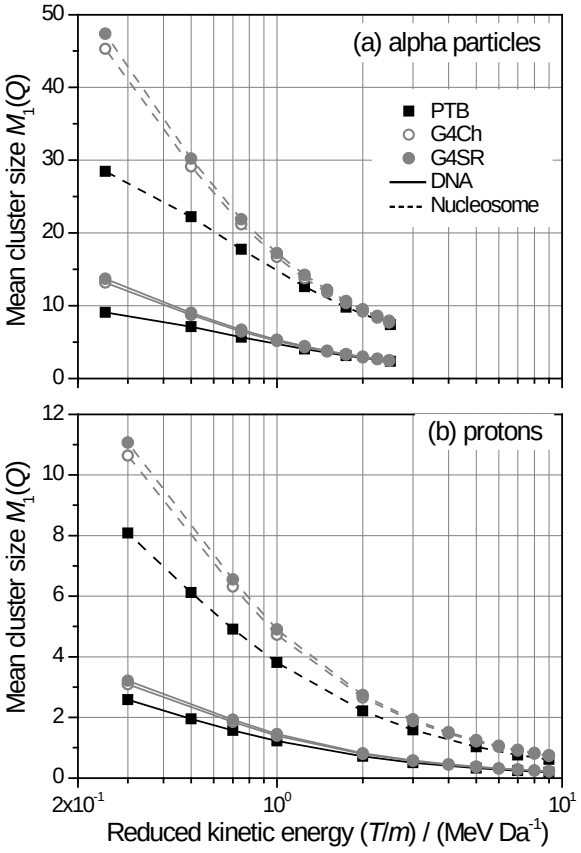

Figure 9. Mean cluster size, $M_1(Q)$, as a function of reduced kinetic energy for incident and alpha particles (a) and protons (b), obtained in the DNA segment and the nucleosome by means of Geant4-DNA and PTB MC code.

The largest differences between Geant4-DNA and PTB codes are seen in the lower part of the energy ranges tested for the particles. This is where the interaction cross sections, particularly for ionisation and charge change processes, are more complex and therefore larger differences between existing theoretical and semi empirical models are to be expected.

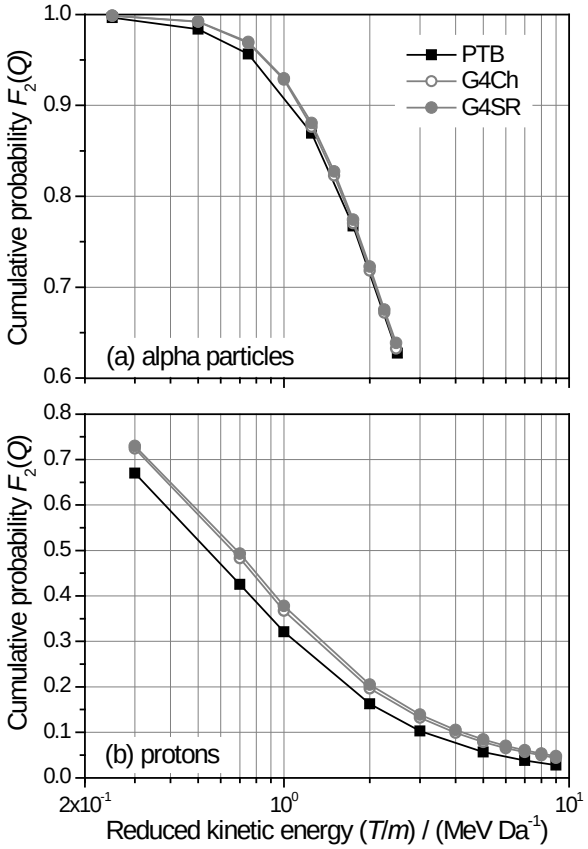

Figure 10. Cumulative probability to produce at least two ionisations within the DNA segment, $F_2(Q)$, as a function of reduced kinetic energy for alpha particles (a) and protons (b) calculated by means of PTB and Geant4-DNA MC codes.

In good agreement with the mean cluster size, $F_2(Q)$ is highest for the lowest primary particle energies available in the PTB code (Figure 10). It decreases for the entirety of the tested energy range. Again, we can see that both Geant4-DNA models for elastic scattering produce very similar results. For protons, consistently smaller $F_2(Q)$ values are seen for the PTB code throughout the whole energy range. This results from the smaller probability, $P(\nu|Q)$, of clusters of size 2 or greater obtained by the PTB code compared to Geant4-DNA, as seen in Figure 8. For alpha particles, the $F_2(Q)$ values obtained by means of the PTB code match well to the Geant4-DNA data, with the results from the PTB code tending to be slightly lower for energies between 2 MeV and 5 MeV. Initially this may not be expected, considering the differences in ionisation

cluster size probability distributions seen in Figure 7. However, $F_2(Q)$ being a cumulative quantity, it is reasonable that such behaviour should be observed. For all alpha particle energies, the PTB code gives a higher maximum in the probability distribution $P(\nu|Q)$, which would significantly increase the value of $F_2(Q)$, whereas Geant4-DNA produces larger cluster sizes which increase the value of $F_2(Q)$ as well. From this comparison of the $F_2(Q)$ values one may expect, for a given radiation quality, that the biological damage predicted by the two codes would therefore be very similar.

It can be seen from Figure 11 that even though there are significant differences between the ionisation probability distributions, these differences have a relatively minor, though still significant, effect on the SB distributions. This implies that the two codes will predict only slightly different amounts of biological damage, despite the presence of particular differences observed between the nanodosimetric track structure quantities obtained by the two codes. This is analogous to the results for primary electrons, where the large differences observed for large ionisation cluster sizes had only a small impact on the SB distribution. For protons, those large ionisation cluster size probabilities are very low (around 10^{-4} and lower), and therefore have only a small effect on the strand break formation. For alpha particles there is a greater difference between the ionisation cluster size distributions and this is translated in to a larger difference in the SB distributions. This is to be expected as there are large differences between the ionisation cluster size distributions even for cluster sizes of high probability (i.e. exceeding 1 %).

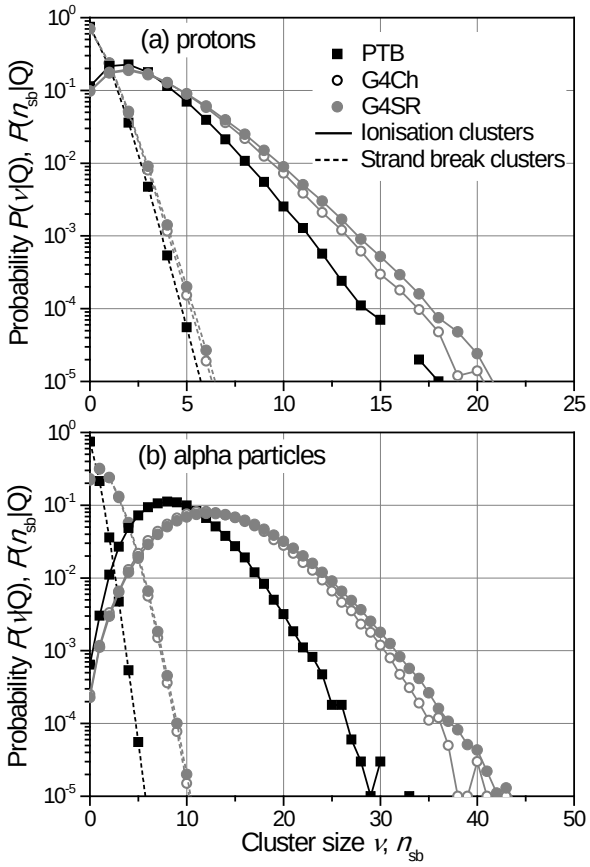

Figure 11. Probability distribution of ionisation cluster size and DNA strand breaks in the DNA segment for 300 keV protons (a) and 1 MeV alpha particles (b), calculated by means of the PTB and Geant4-DNA MC codes.

As a further investigation to characterise the two codes for nanodosimetry applications, we compared the probability of producing a DSB as described in Section 2.1. Generally, the probability of DSB formation is seen to decrease with increasing primary particle energy (Figure 12). The reason for this is that, in the energy ranges investigated here, the LET of the two particle types, and therefore the number of ionisations in the DNA segment, decreases with increasing energy. The relative differences seen here are around 40 % for low proton energies (P(DSB|Q) around 3.1 % for Geant4 and 2.2 % for the PTB code). For alpha particles the Geant4-DNA data consistently predicted a higher probability (between 10 % and 70 % relative increases) of producing a DSB than the PTB data. Consequently, the amount of biological damage predicted by Geant4-DNA will be significantly greater than that predicted by the PTB

code, particularly for lower energies of both particles. This is in contrast with the $F_2(Q)$ values that were generally equal for both codes (Figure 10).

The reason for this is that at least two strand breaks must occur for a DSB to be produced, so that the contribution of larger ionisation cluster sizes is increased compared to smaller ones when determining $P(\text{DSB}|Q)$ as described in equations 4 and 5. For protons the differences between the codes is greater for larger clusters which increases the differences in the number of SB (as seen in Figure 11) and, subsequently, the differences between the DSB probability predictions of the two codes. For alpha particles, instead, the probability of producing a very small ionisation cluster size compares to the probability of producing a very large cluster size. However, a very large ionisation cluster size is more likely to result in complex damage to the DNA molecule (complex DSB) than a very small number of ionisations. While this will have a significant effect on the calculation of $P(\text{DSB}|Q)$, it will not significantly influence the value of $F_2(Q)$.

This means that the DSB probability will be particularly sensitive to differences in ionisation cluster size distributions, implying that $P(\text{DSB}|Q)$ is highly dependent on the track structure of the radiation.

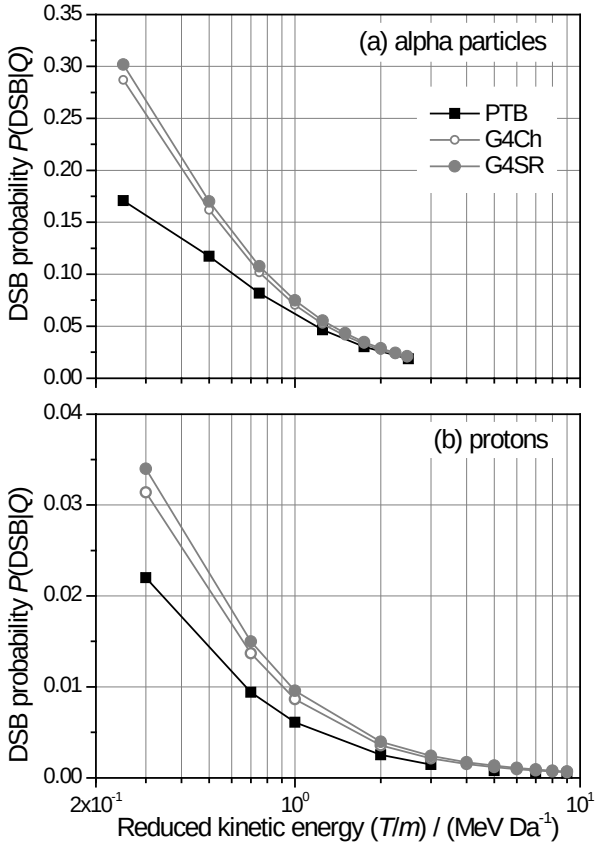

Figure 12. Probability of producing a DSB for alpha particles (a) and protons (b), calculated by means of the PTB and Geant4 MC codes using the Champion model for elastic scattering.

4. CONCLUSION

The aim of this paper was to quantitatively compare several nanodosimetric parameters calculated using Geant4-DNA and the PTB Monte Carlo track structure code in order to assess the effect of using different transport methods and different physical interaction cross sections on these quantities. We simulated the transport of pencil beams of monoenergetic particles (electrons, protons and alpha particles) inside nanometric-sized volumes equivalent to a DNA segment and a nucleosome.

We found that there is generally good agreement between Geant4-DNA and the PTB MC code regarding NPTS, particularly in the higher energy range. The discrepancies that we observed (up

to 25 % for track structure parameters) in the lower energy range are presumably due to the different physical interaction cross sections used in the two codes. The largest differences are obtained at energies where the LET is higher and more interactions take place.

For electrons, the difference between the two codes is largest below 300 eV, with Geant4-DNA systematically showing a higher number of ionisations produced in the sensitive volume. For light ions, the results show that a higher number of ionisations in the sensitive volumes is obtained when using Geant4-DNA, particularly for low energies, which in this case corresponds to higher LET values. These discrepancies are most likely due to differences in the impact ionisation cross sections of the primary particles, since the number of ionisations produced by secondary electrons is small compared to those produced by the primary protons or alpha particles. Therefore the influence of different electron transport models used in the codes is of relatively minor importance for ion track structure parameters.

Three different nanodosimetric estimators for biological effectiveness have been calculated from the simulated ionisation cluster size distributions: Cumulative probability $F_2(Q)$ for ionisation cluster sizes larger than 1, probability distributions $P(n_{sb}|Q)$ for strand break cluster size n_{sb} and the overall probability for DSB induction, $P(\mathrm{DSB}|Q)$. For electrons, the nanodosimetric estimates of biological effectiveness determined with the two codes are in good agreement for energies above 200 eV and show differences up to a factor of 2.5 below that energy. Proton data show significant differences of more than 40 % in DSB probabilities over the entire energy range tested. Alpha particle data also show large differences, of over 60 % in $P(\mathrm{DSB}|Q)$. For both ion types, Geant4-DNA gives higher probability of producing a DSB than the PTB code across the entire energy range. A similar trend is seen for the cumulative probability for ionisation clusters of size two or more, $F_2(Q)$. However, here the results of the two codes show only minor discrepancies for alpha particles whereas the relative difference amounts to up to 5% for protons.

While the discrepancies found in this work are still within the uncertainty limits usually considered in radiation protection, significant improvement is required for applications of computational nanodosimetry in radiotherapy in terms of chosen MC code and for establishing the correlation of nanodosimetric characteristics of track structure and in vivo biological cell killing.

ACKNOWLEDGEMENTS

This work was supported by the CMRP University of Wollongong, Australia and PTB, Germany.

Appendix

Details on the track structure Monte Carlo simulations

Both the PTB MC code and Geant4-DNA use the same general procedure for track structure simulation: single interactions are directly random sampled according to the relative magnitude of the respective total physical interaction cross sections as mentioned in the introduction. Those are ionisation, excitation and elastic scattering for electrons, and ionisation, excitation and charge exchange for protons and alpha particles (including interaction cross sections for H^+, H^0, He^0, He^+, He^{2+}). When the energy of the primary particle falls below a given lower limit, the particle is assumed to locally deposit all its remaining energy at the site where the last interaction occurred. Its secondary electrons are subsequently transported in a similar manner. The lower energy limit for electrons in Geant4-DNA is 8.23 eV for the excitation and elastic scattering models (Incerti *et al* 2010), while the threshold of ionisation is fixed at 12.61 eV (Chauvie *et al* 2007). In the PTB code, the cut off limit for the lower electron energy is set to 10.79 eV (Grosswendt 2005). Protons and alpha particles can be followed down to a lower energy limit of 100 eV in Geant4, while the PTB code does rely on the accuracy of its incorporated physical models down to 300 keV for protons or 1 MeV for alpha particles.

The accuracy of the Monte Carlo simulation depends strongly on the physical models for electromagnetic interaction cross sections, applied to describe the particle interactions in the medium of interest. Commonly, in Monte Carlo simulations, interaction cross sections for liquid water are used as an approximation for biological material. In contrary to low-density material in the gas phase, where interaction cross sections can be experimentally determined with sufficient accuracy, those in liquid water cannot be measured directly, due to the inability of the incoming particle to experience only a single interaction in the medium. While a tracking of high energetic particles can still be achieved with sufficient accuracy also for condensed material by using the

Bethe-Born theory, the interactions of low energetic particles with the target molecules are more complex.

For electrons, various theoretical models exist (Dingfelder *et al.* 1998, Emfietzoglou and Nikjoo 2005, Champion 2003, Rudd 1991, Kutcher and Green 1976), however, they show differences already for the total, inelastic and elastic cross sections of electrons below 1 keV. Most of the authors derived their inelastic cross sections on the basis of optical measurements on liquid water by Heller *et al* (1974). These experimental data allow only the direct calculation of the optical oscillator strength and therefore, of interactions at the dipole limit. The Sendai group (Hayashi *et al.* 2000), on the other hand, derived a large range of the generalized oscillator strength from x-ray scattering experiments, which enable a calculation of the inelastic cross sections with greater accuracy (Emfietzoglou and Nikjoo 2005). Other groups use quantum mechanical calculations to determine the interaction cross sections (Rudd 1991, Champion 2003.). A detailed comparison of the existing interaction cross sections for electrons can be found in (Champion 2003, Emfietzoglou *et al.* 2009). Regarding the treatment of inelastic scattering in the Monte Carlo codes used in this study, the model developed by Emfietzoglou *et al* (Emfietzoglou and Nikjoo 2005) was applied in Geant4-DNA. The PTB code, on the other hand, is based on the energy loss functions derived by Dingfelder *et al.* (1998) from measured data of Grosswendt and Waibel (1978) and used the semi-empirical model of Green and Sawada (1972) for excitation as parameterized by Kutcher and Green (1976). Elastic scattering, which is commonly neglected for high particle energies, is the dominant interaction in the low energy regime for electrons. Both codes use modified screened-Rutherford models to calculate the total elastic cross section as well as the scattering angle for electron energies above 200 eV and the semi-empirical model of Brenner and Zaider (1983) below. Geant4-DNA offers an alternative analytical model developed by Champion (Champion 2003), which takes also polarization and exchange effects in the low energy domain into account.

For protons and alpha particles the inelastic cross sections contained in Geant4-DNA are calculated by the Bethe-Born theory for energies greater than 500 keV. Below, a semi-empirical model is used to treat ionisations (Dingfelder *et al.* 2000). Excitations are calculated using the model developed by Miller and Green (1973) for both, Geant4-DNA and the PTB code. The total inelastic ion cross sections for ions applied in the PTB code are based on the analytical model developed by Rudd *et al*. (1985) and the differential ionisation cross sections are obtained from the model of Hansen and Kocbach (ICRU 1996).

REFERENCES

Agostinelli S, Allison J, Amako K, Apostolakis J, Araujo H, Arce P, Asai M, Axen D, Banerjee S, Barrand G *et al* 2003 GEANT4-a simulation toolkit *Nucl. Instr. and Meth. A* **506** 250-303

Allison J, Amako K, Apostolakis J, Araujo H, Dubois P A, Asai M, Barrand G, Capra R, Chauvie S, Chytracek R *et al* 2006 Geant4 developments and applications *IEEE Trans. Nucl. Sci.* **53** 270-8

Bashkirov V, Schulte R, Wroe A, Sadrozinski H, Gargioni E and Grosswendt B 2009 Experimental Validation of Track Structure Models *IEEE Trans. Nucl Sci* **56** 2859-63

Bedford J S 1991 SUBLETHAL DAMAGE, POTENTIALLY LETHAL DAMAGE, AND CHROMOSOMAL-ABERRATIONS IN MAMMALIAN-CELLS EXPOSED TO IONIZING-RADIATIONS *Int. J. Radiat. Oncol. Biol. Phys.* **21** 1457-69

Berger M J, Coursey J S, Zucker M A and Chang J 2005, ESTAR, PSTAR, and ASTAR: Computer Programs for Calculating Stopping-Power and Range Tables for Electrons, Protons, and Helium Ions (version 1.2.3). [Online] Available: http://physics.nist.gov/Star [2010, *September 13*]. National Institute of Standards and Technology, Gaithersburg, MD.

Brenner D J and Zaider M 1983 A computationally convenient parameterisation of experimental angular distributions of low energy electrons elastically scattered off water vapour *Phys. Med. Biol.* **29** 443–47

Bug M U, Gargioni E, Guatelli S, Incerti S, Rabus H, Schulte R and Rosenfeld A B 2010 Effect of a magnetic field on the track structure of low-energy electrons: a Monte Carlo study, *Eur. Phys. J. D* **60** 85 - 92

Champion C 2003 Theoretical cross sections for electron collisions in water: structure of electron tracks *Phys. Med. Biol.* **48** 2147-68

Chauvie S, Francis Z, Guatelli S, Incerti S, Mascialino B, Montarou G, Moretto P, Nieminen P and Pia M G 2006 Monte Carlo simulation of interactions of radiation with biological systems at the cellular and DNA levels: The Geant4-DNA project *Radiat. Res.* **166** 676-7

Chauvie S, Francis Z, Guatelli S, Incerti S, Mascialino B, Moretto P, Nieminen P and Pia M G 2007 Geant4 physics processes for microdosimetry simulation: Design foundation and implementation of the first set of models *IEEE Trans. Nucl. Sci.* **54** 2619-28

Dingfelder M, Hantke D, Inokuti, M and Paretzke H G 1998 Electron inelastic-scattering cross sections in liquid water *Radiat. Phys. Chem.* **53** 1–18

Dingfelder M, Inokuti M and Paretzke H G 2000 Inelastic-collision cross sections of liquid water for interactions of energetic protons *Radiat. Phys. Chem.* **59** 255–275

Dingfelder M, Ritchie R H, Turner J E, Friedland W, Paretzke H G and Hamm R N 2008 Comparisons of calculations with PARTRAC and NOREC: Transport of electrons in liquid water *Radiat. Res.* **169** 584-94

Emfietzoglou D, Garcia-Molina R, Kyriakou I, Abril I and Nikjoo H 2009 A dielectric response study of the electronic stopping power of liquid water for energetic protons and a new I-value for water *Phys. Med. Biol.* **54** 3451–72

Emfietzoglou D and Nikjoo H 2005 The effect of model approximations on single-collision distributions of low-energy electrons in liquid water *Radiat. Res.* **163** 98–111

Friedland W, Jacob P, Paretzke H G, Merzagora M and Ottolenghi A 1999 Simulation of DNA fragment distributions after irradiation with photons *Radiat. Environ. Biophys.* **38** 39-47

Gargioni E and Grosswendt B 2007 Influence of ionization cross-section data on the Monte Carlo calculation of nanodosimetric quantities *Nucl. Instr. and Meth. A* **580** 81-4

Garty G, Schulte R, Shchemelinin S, Grosswendt B, Leloup C, Assaf G, Breskin A, Chechik R and Bashkirov V 2006 First attempts at prediction of DNA strand-break yields using nanodosimetric data *Radiat. Prot. Dosimetry.* **122** 451-4

Garty G, Schulte R, Shchemelinin S, Leloup C, Assaf G, Breskin A, Chechik R, Bashkirov V, Milligan J and Grosswendt B 2010 A nanodosimetric model of radiation-induced clustered DNA damage yields *Phys. Med. Biol.* **55** 761-81

Goodhead D T 1994 INITIAL EVENTS IN THE CELLULAR EFFECTS OF IONIZING-RADIATIONS - CLUSTERED DAMAGE IN DNA *Int. J. Radiat. Biol.* **65** 7-17

Goodhead D T 2006 Energy deposition stochastics and track structure: What about the target? *Radiat. Prot. Dosimetry* **122** 3-15

Goodhead D T, Thacker J and Cox R 1993 EFFECTS OF RADIATIONS OF DIFFERENT QUALITIES ON CELLS - MOLECULAR MECHANISMS OF DAMAGE AND REPAIR *Int. J. Radiat. Biol.* **63** 543-56

Green, A E S and Sawada, T 1972 Ionization cross sections and secondary electron distributions *J. Atmos. Terr. Phys.* **34** 1719–28

Grosswendt B 2002 Formation of ionization clusters in nanometric structures of propane-based tissue-equivalent gas or liquid water by electrons and alpha-particles *Radiat. Environ. Biophys.* **41** 103-12

Grosswendt B 2004 Recent advances of nanodosimetry *Radiat. Prot. Dosimetry* **110** 789-99

Grosswendt B 2005 Nanodosimetry, from radiation physics to radiation biology *Radiat. Prot. Dosimetry* **115** 1-9

Grosswendt B 2006 Nanodosimetry, the metrological tool for connecting radiation physics with radiation biology *Radiat. Prot. Dosimetry* **122** 404-14

Grosswendt B and Pszona S 2002 The track structure of alpha-particles from the point of view of ionization-cluster formation in "nanometric" volumes of nitrogen particles *Radiat. Environ. Biophys.* **41** 91-102

Grosswendt B and Waibel E 1978 Transport of low energy electrons in nitrogen and air *Nuc. Instr. Meth.*, **155** 145-56

Grosswendt B, Pszona S and Bantsar A 2007 New descriptors of radiation quality based on nanodosimetry, a first approach biology *Radiat. Prot. Dosimetry* **126** 432-44

Guatelli S, Mascialino B, Moneta L, Papadopoulos I, Pfeiffer A, Pia M G and Piergentili M 2004 *2004 IEEE Nuclear Science Symposium Conference Record, Vols 1-7*, ed J A Seibert pp 2100-3

ICRU 1996. Secondary electron spectra from charged particle interactions *International Commission on Radiation Units and Measurements (Bethesda, Maryland, USA), ICRU Report* **55** 51–2

Hayashi H, Watanabe N, Udagawa Y and Kao C-C 2000 The complete optical spectrum of liquid water measured by inelastic x-ray scattering *PNAS* **97** 6264–66

Heller J M, Hamm R N, Birkhoff R D and Painter L R 1974 Collective oscillation in liquid water *J. Chem. Phys.* **60** 3483–86

Incerti S, Ivanchenko A, Karamitros M, Mantero A, Moretto P, Tran H N, Mascialino B, Champion C, Ivanchenko V N, Bernal M A, Francis Z, Villagrasa C, Baldacchino G, Gueye P,

Capra R, Nieminen P and Zacharatou C 2010 Comparison of GEANT4 very low energy cross section models with experimental data in water *Med. Phys.* **37** 4692-708

Krämer M, Kraft G 1994, Calculations of heavy-ion track structure *Radiat. Environ. Biophys.* **33** 91-109

Kutcher G J and Green A E S 1976 A model for energy deposition in liquid water *Radiat. Res.* **67** 408–25

Miller J H and Green A E S 1973 Proton energy degradation in water vapour *Radiat. Res.* **54** 343–63

Nikjoo H and Goodhead D T 1991 TRACK STRUCTURE-ANALYSIS ILLUSTRATING THE PROMINENT ROLE OF LOW-ENERGY ELECTRONS IN RADIOBIOLOGICAL EFFECTS OF LOW-LET RADIATIONS *Phys. Med. Biol.* **36** 229-38

Nikjoo H, O'Neill P, Goodhead D T and Terrissol M 1997 Computational modelling of low-energy electron-induced DNA damage by early physical and chemical events *Int. J. Radiat. Biol.* **71** 467-83

Nikjoo H, Uehara S, Emfietzoglou D and Cucinotta F A 2006 Track-structure codes in radiation research *Rad. Meas.* **41** 1052-1074

Rabus H, Nettelbeck H 2011 Nanodosimetry: bridging the gap to radiation biophysics, *Radiat. Meas.* in press. DOI: 10.1016/j.radmeas.2011.02.009

Rudd M E 1991 Secondary electrons from charged particle collisions with atoms and molecules *Nuc. Instrum. Meth. Phys. Res. B* **56/57** 162–165

Rudd M E, Kim Y-K, Madison D H and Gallagher J W 1985 Electron production in proton collisions: total cross sections *Rev. Mod. Phys.* **57** 965–94

Salvat F, Fernández-Varea J, Sempau J 2006, *Penelope-2006: A Code System for Monte Carlo Simulation of Electron and Photon Transport,* Nuclear Energy Agency, viewed 12 January 2011, http://www.oecd-nea.org/html/science/pubs/2006/nea6222-penelope.pdf

Schulte R W, Wroe A J, Bashkirovz V A, Garty G Y, Breskin A, Chechik R, Shchemelinin S, Gargioni E, Grosswendt B and Rosenfeld A B 2008 Nanodosimetry-based quality factors for radiation protection in space *Z. Med. Phys.* **18** 286-96

Valota A, Ballarini F, Friedland W, Jacob P, Ottolenghi A and Paretzke H G 2003 Modelling study on the protective role of OH radical scavengers and DNA higher-order structures in induction of single- and double-strand break by gamma-radiation *Int. J. Radiat. Biol.* **79** 643-53

Wichmann B A and Hill I D 1982 AN EFFICIENT AND PORTABLE PSEUDO-RANDOM NUMBER GENERATOR *J. Roy. Stat. Soc. C Appl. Stat.* **31** 188-90